The pulse-elevator: A pump for granular materials

Xuan Li, Kevin Worrall, Aditya Vedanthu, Andrew Scott-George, Patrick Harkness [*]

James Watt School of Engineering, University of Glasgow, UK

ARTICLE INFO

ABSTRACT

Granular materials include fuels, foods, feedstocks, and raw materials, and they are frequently created in drilling, exploration, and comminution. However, despite this ubiquity, they can be much more difficult to transport than other materials. Screw conveyors can be used, as can bailing, gas-blowing, and vibro-conveyors, but all have issues related to some combination of complexity, inclination, differential friction, and torque reaction. We propose an entirely new concept: a combination of the vibro-conveyor and the Tesla valve. This 'pulse-elevator' is a single piece of inert material, it can operate vertically, it does not depend upon frictional interactions, and it is effectively torqueless. This paper describes the mechanism in analytical, numerical, and experimental terms, and then illustrates two successful experimental use cases: powder uplift from a hopper, and the replacement of augering in a rock-drilling application. These cases are particularly relevant for the facilitation of ISRU and subsurface exploration in space.

1. Introduction

Screw conveyors, first reported by Archimedes in 234 BC, can uplift granular materials along an inclined plane. Our technical understanding [1] and practical implementation of this technique continue to improve, with increased flexibility [2] providing a route for development into more compliant systems. However, as with many rotating systems, they can require a starting torque far in excess of steady-state [3].

As the inclination angle increases towards the vertical, the operating mechanism changes. Instead of having the spoil material on only the lower side of the surrounding tube, it becomes evenly distributed and conveying gives way to augering. This mechanism requires differential friction between the granular material and the two working surfaces, namely the flights and the surrounding tube, which increases the torque requirement. Linked limitations on flight angle, minimum diameter, and rotation speed begin to emerge [4]. Extant alternatives to augering, for vertical transport, include pneumatic conveying (which requires a working fluid), bailing (which requires complex mechanical support), and bristle-based systems (which require relatively-moving parts downhole) [5].

The vibro-conveyor, on the other hand, uses a complex vibrational pattern to cause a particle to break contact with an inclined plane, fly a short trajectory, and touchdown further up the same inclined plane [6]. In an improvement over augering and bailing, the need for relative movement between different parts of the system is eliminated. However, the particle-surface friction remains crucial, so shock is poorly tolerated and the inclination angle remains constrained. Vertical transport may be approximated by winding the conveyor into a helix, but this is a bulky and inflexible solution.

In the context of space exploration, variations on the auger are a crucial part of many In-Situ Resource Utilisation (ISRU) concepts due to its relatively low diameter and its ability to carry out a vertical uplift, despite its high torque requirements and other operational issues [7]. For example, jamming can occur when the flights of an auger are entirely choked with material such that flow becomes impossible, although this problem can sometimes be cleared by reversing the auger. Starvation, on the other hand, occurs when the auger works correctly, but insufficient material is entrained. Powdery materials can cake around the auger intakes, such that no more will fall into the ports which accept material into the flights. If sufficient space is available, a stirrer can agitate the material and help to keep the auger in action [8].

A key test for an alternative to the traditional auger architecture is therefore to determine if it can uplift a granular material from a hopper without jamming or starvation. This experiment is undertaken as part of the first use case considered in this paper, and the pulse-elevator concept appears to demonstrate functionality in this application.

Augers have also been a part of every deep-drilling campaign so far attempted in hard materials. This is again due to their relatively low diameter, their vertical aspect, and their shock tolerance which ensures that they remain compatible with percussive drilling. On the moon, the

---
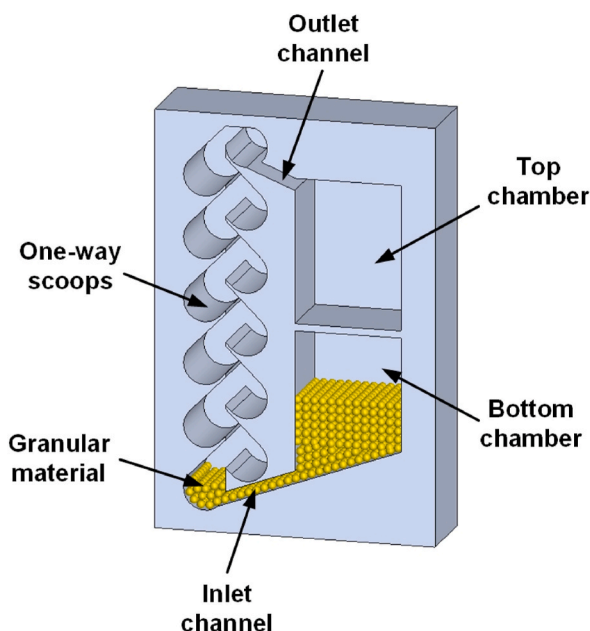
Fig. 1. A pulse-elevator test piece, which is vibrated in the vertical direction to pump the particles upwards.

Fig. 2. The inertial trajectory of a single particle (red) attempting to reach the position of the scoop above (blue). The hop is only just successful, so this is the limiting 'saturation' state. The capture event itself is not modelled: in reality, the particle would conform to the position history of the scoop from ~0.06s onwards. (For interpretation of the references to colour in this figure legend, the reader is referred to the Web version of this article.)

Apollo astronauts used an augering drill [9], as have all relevant robotic expeditions: Luna 16 used an auger in 1970 [10], with Chang'e 5 using the fundamentally the same concept fifty years later [11]. The ProSEED augering drill was intended to fly on Luna 27 [12], and alternatives are now being matured for the future. On Venus, the Venera landers were equipped with augering drills [13]. Mars has already seen the augering drill of Perseverance [14], and the ExoMars augering drill is planned [15]. Even comets have been addressed with an auger, via the Rosetta SD2 drill [16]. In all cases, these missions have been challenged to rotate an auger against the friction of the borehole walls. This friction generates a torque, which is difficult to react from a lightweight lander in a low gravity field. As a result, borehole depths have been constrained and no robotic mission has been able to penetrate beyond a few hundred mm without employing a very large landed mass, as was the case for the Luna drilling/sampling missions. A new torqueless technology for accessing hard materials, independent of the inevitably-lossy friction uplift mechanism, would therefore have great potential in this domain.

The supplementary test for any new architecture is therefore to determine if it can be incorporated into a percussive drillbit that can penetrate a hard material to a considerable depth. This is examined as part of the second use case in this paper, where a drillbit is used to penetrate a block of volcanic tuff and bring the spoil to the surface. In this experiment the drillbit is dithered back-and-forth to prevent imprintation of the cutting bit, but this is emphatically not an augering motion: a bare minimum of rotational speed is required, there is no gross rotation, and there is negligible friction against the walls. Again, the pulse-elevator demonstrated a high degree of functionality in this application.

The pulse-elevator achieves these outcomes by developing the Tesla valve [17] for granular materials, and adding a reciprocating motion similar to, but simpler than, the motion of a vibro-conveyor. The device uses opposing scoops which prevent particles from falling – even under shock – but which present little obstacle to upwards motion. When the device is vibrated at an intensity that significantly exceeds $\Gamma = 1$, where the relative acceleration $\Gamma = A\omega^2/g$ [18], the contents of each scoop are projected upwards and are deflected (without a friction requirement) into the opposing scoop on the other side of the device, where the cycle repeats. Each scoop ejects its contents into the opposing scoop above, just before it is refilled by the opposing scoop below. The vibration
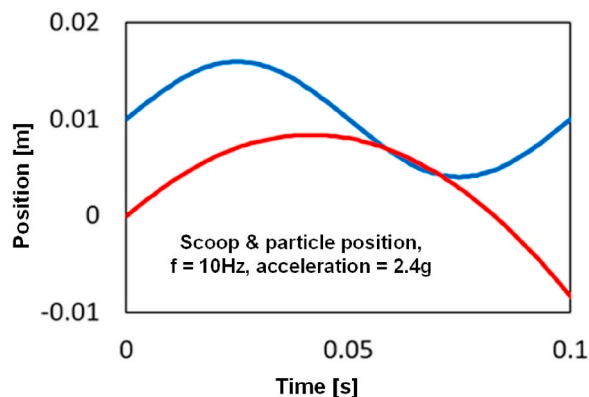
pattern required is not tightly defined, in contrast to the vibro-conveyor, because a sinusoidal motion (or indeed, almost any oscillating motion) is perfectly adequate.

Fig. 1 shows a simple testbed for this device. Granular material is placed in the bottom chamber, which feeds downhill into the pulse-elevator geometry. With each vibration cycle of sufficient magnitude, the particles may hop up and over into the next opposing scoop, above their starting point, until they reach the top of the elevator. They will then feed downhill into the top chamber. This geometry and behaviour is highly robust to minor deviations in execution, so a test piece can easily be 3D printed and verified by the reader (see Appendix).

2. Design of the investigation

The performance of this device will be analysed from an analytical, numerical, and experimental standpoint using 1 mm spheres, with glass spheres being used for the practical case. Two application cases will then be tested: the uplift of graded block paving sand from a hopper, and the extraction of spoil from the bottom of a hole drilled by a percussive penetrator equipped with an internal pulse-elevator. The hole will be drilled in volcanic tuff.

3. 1-D analytical model of the experiment

The behaviour of the pulse-elevator can be simplified if only a single particle is considered, with positive defined as upwards. Then, using the equations of harmonic motion, the position, velocity, and acceleration histories of the device can be calculated in the inertial frame. The instantaneous acceleration of the device is zero as it rises through the neutral plane, but it becomes increasingly negative immediately thereafter. As the device passes through −1 g, any particle within the device is assumed to become free-flying with the (still-upwards) velocity of the device at the instant of take-off, but with a (naturally downwards) acceleration due to gravity.

In the device frame, the particle must use its ballistic flight to climb through the hop distance from one scoop to the lip of the next (10 mm, in the geometry tested), being deflected sideways towards its target as required (although, in this analytical investigation, this motion is disregarded). Fortunately, in the inertial frame, the particle need not climb the full 10 mm because the device will move downwards on its next cycle, closing some of the gap. It is a simple matter to propagate the movements to determine the oscillation parameters which permit successful hopping. The harmonic acceleration which just permits a successful hop by any particle in any scoop is termed the 'saturation'

Table 1
Simulated activation and saturation excitations, with 10 mm scoop spacing.

Frequency (Hz)	10	20	30	40	50
Activation acceleration (g)	1.9	3.3	5.2	7.6	10.9
Saturation acceleration (g)	2.4	4.8	8.2	13.1	19.4

excitation.

However, with bulk particles, the scoops are generally approximately half-full. This means that any one particle on top of the others does not have to hop so high to make it into the next scoop, even if the particles below are left behind. If the lower 5 mm of the scoop is already filled with material, then the minimum hop distance will be reduced to the outstanding 5 mm, to make up the 10 mm total. We term the lower acceleration required to close this smaller gap the 'activation' excitation, because it marks the beginning of functionality.

An example is given in Fig. 2. In this case, the simulation time starts as the device moves upwards through the midpoint, with a particle at position 0 and the lip of the next scoop 0.01 m higher. This particle (red history) initially follows the harmonic motion of the device, but becomes free-flying at 0.007 s. The scoop immediately above (blue history) continues its harmonic motion, such that at 0.06 s, the near-hovering particle may be (just) caught by the rapidly descending scoop. This simulation does not, however, model the 'capture' event, so the red
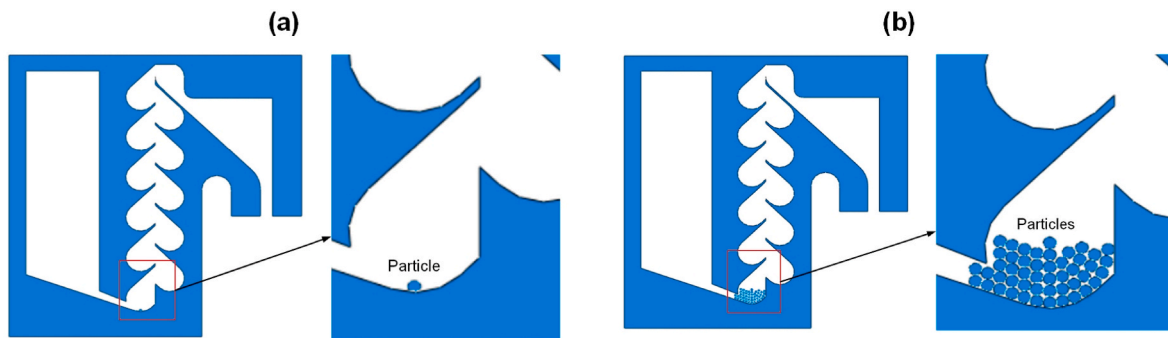

Fig. 3. (a) single-particle 2-D finite element model, (b) multi-particle 2-D finite element model.
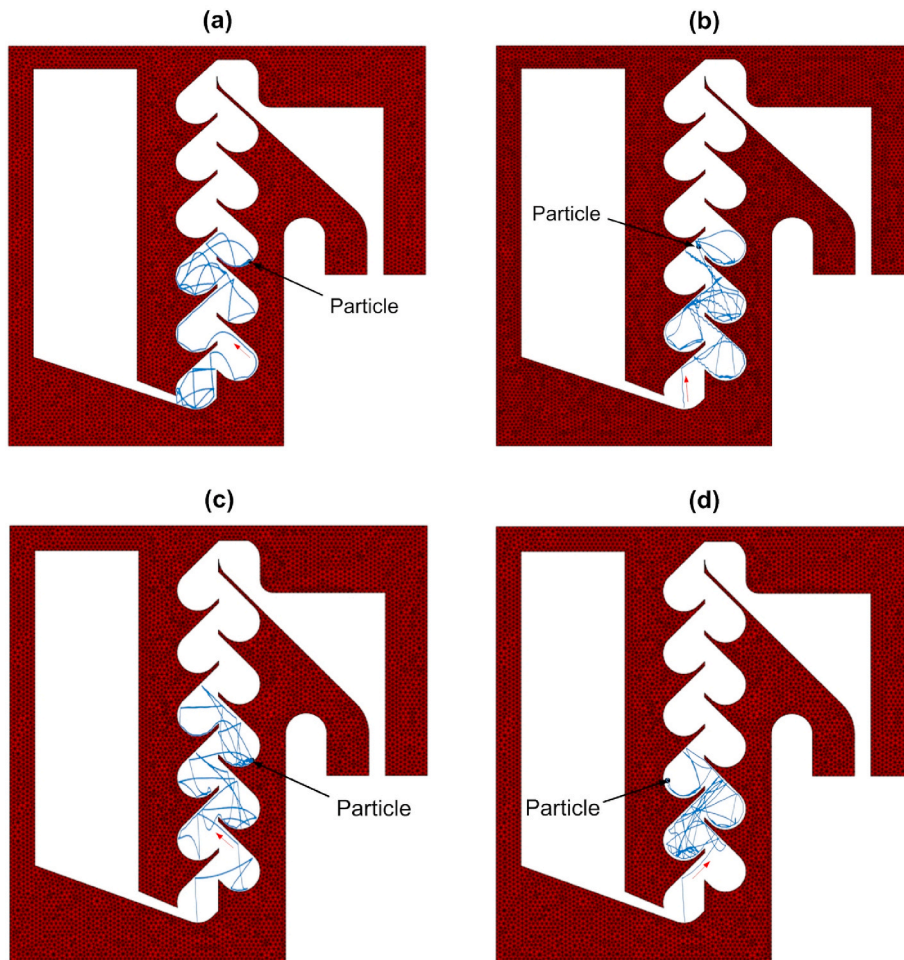

Fig. 4. The local trajectory of a single particle during 1 s of excitation, at: (a) 2 g, (b) 3 g, (c) 4 g, and (d) 5 g. The 1 g case is not shown, as the particle simply remained within the lowest scoop.
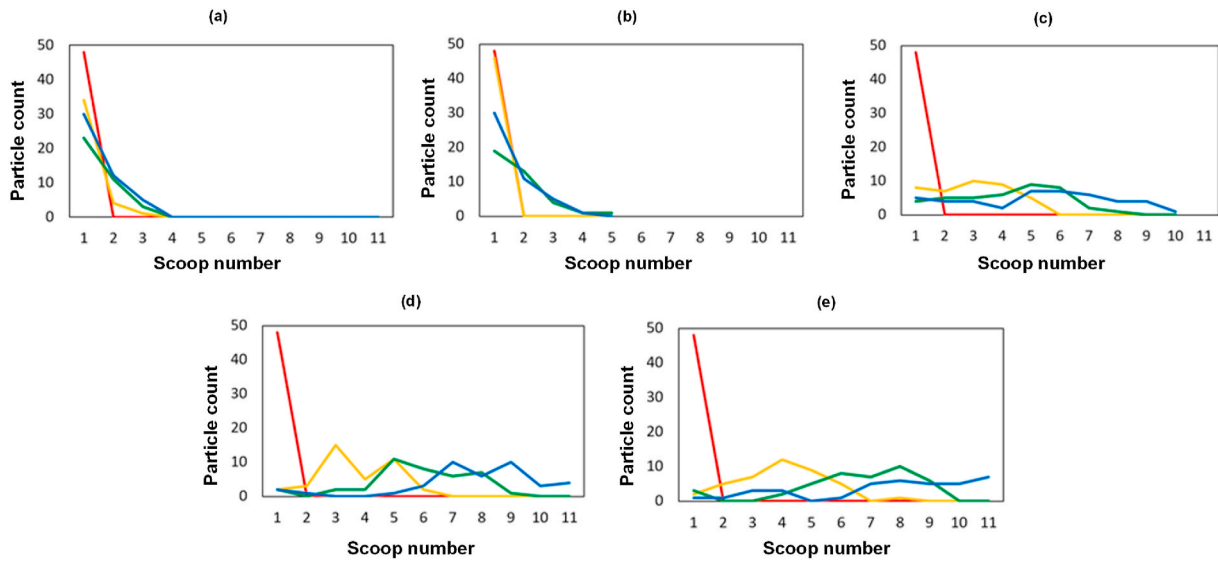
Fig. 5. Particle distribution after 0 s (red), 0.3 s (orange), 0.6 s (green), and 0.9 s (blue), at 10 Hz and various gravity levels: (a) 1 g, (b) 2 g, (c) 3 g, (d) 4 g, (e) 5 g. (For interpretation of the references to colour in this figure legend, the reader is referred to the Web version of this article.)
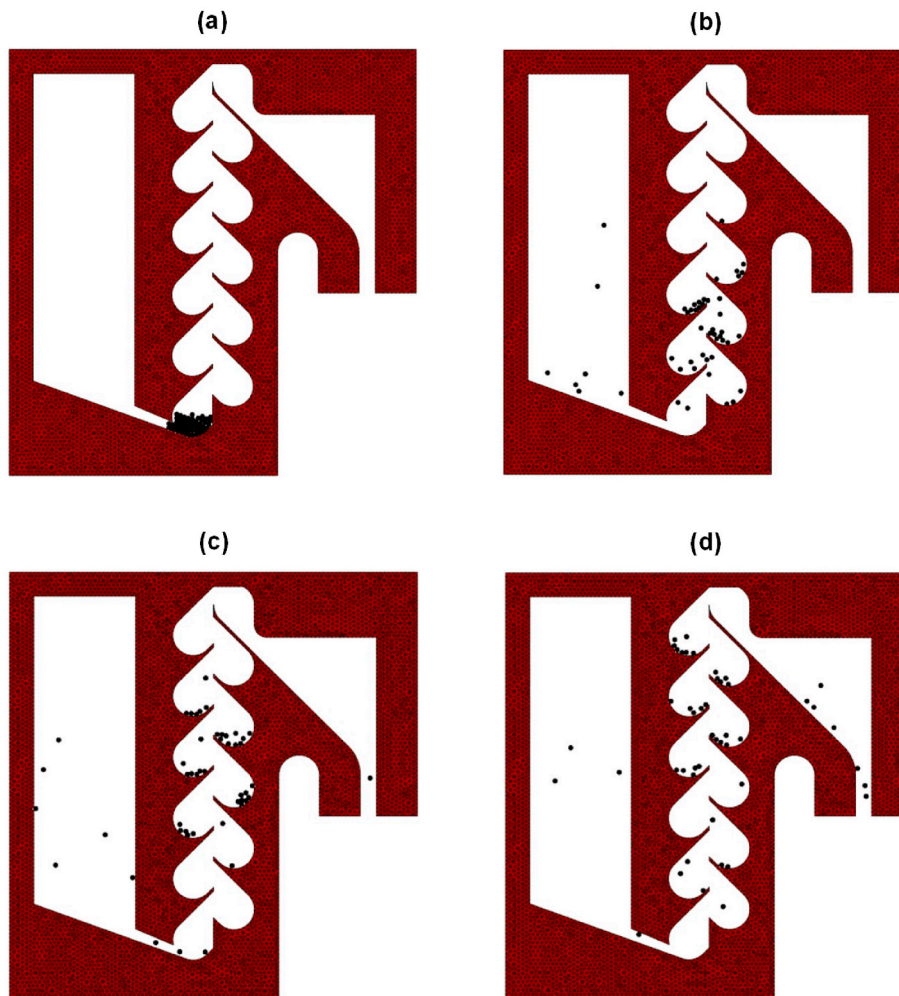

Fig. 6. Particle distribution, at: (a) 0 s, (b) 0.3 s, (c) 0.6 s, and (d) 0.9 s after initialisation at 5 g. Note the number of particles in each scoop, numbered 1 to 11 from the bottom: these counts correspond to the red, orange, green, and blue traces in Fig. 5 (e). (For interpretation of the references to colour in this figure legend, the reader is referred to the Web version of this article.)

history continues under its own inertia. Obviously, some small horizontal movement would also be needed to make the capture in reality.

This simplified model can predict the 'activation' acceleration where particles begin to climb and the 'saturation' acceleration where each scoop can be fully emptied. These are given in Table 1, and the values can be divided by g (gravity) to obtain the nondimensional relative acceleration Γ, if so desired. Naturally, these results assume no adhesion to the surfaces, or aerodynamic/electrostatic effects in flight, which might exist in a real-world scenario.

4. Finite element model of the experiment

The device may be simulated in finite element software (Abaqus-Simulia, Dassault Systèmes, Vélizy-Villacoublay, France). To examine the 'activation' and 'saturation' limits, two scenarios are investigated: the first is the analysis of a single particle at various frequencies and accelerations (Fig. 3 (a)), and the second considers that the bottom half of the bottom scoop of the device is filled with particles, and then propagates the chaotic interactions between the particles and walls of the device. This is a somewhat more realistic model of the real world (Fig. 3 (b)).

To reduce computation time, 2-D models are used and only the 10 Hz case is considered. A gravity of 9.81 m/s^2 is assigned, and the device is oscillated with amplitude as a driven parameter. All interactions are assumed to be elastic and frictionless. The surrounding structure (the feed hopper and the output spout) has been modified for experimental purposes, as will be explained in a later section, but this will not affect the dynamics in the scoops.

The single-particle model is excited at 1 g, 2 g, 3 g, 4 g, and 5 g, to find the saturation acceleration (where each particle must hop the full height of every scoop). According to Table 1 the analytical threshold is at 2.4 g, so climbing should be seen in the 3 g case, and thereafter. The actual results, for 1 s of movement, are shown in Fig. 4.

The results show climbing from the 2 g case, which is therefore unexpected, but it appears that energy can be accumulated over a few cycles and then expended in a single, larger movement. An examination of the trajectories at 2 g, 3 g, 4 g, and 5 g – all of which show a net total ascent of between 4 and 6 scoops – suggests that this accumulation, in the context of a single particle in a chaotic system, is a reasonable explanation for the unexpected result.

In the multi-particle simulations we may expect more consistent performance, due to averaged chaos. This is presented in Fig. 5, which considers how many particles are found in each scoop, numbered from #1 at the bottom to #11 at the top, after different periods of time: 0 s of excitation (red), 0.3 s (orange), 0.6 s (green), and 0.9 s (blue).

It is immediately apparent that, as the acceleration is increased, the great bulk of the particles is more effectively moved towards the top of the pulse-elevator as time progresses. In fact, after 1 s, the pulse-elevator operating at 4 g was able to eject four particles past scoop #11, and the pulse-elevator operating at 5 g was able to eject thirteen particles past scoop #11 and into free space. These systems would very likely have cleared all particles in a few more seconds of computation, but the price of executing such an analysis would exceed its informational value.

The performance of the 5 g elevator is shown as an example, in Fig. 6, so that the movement can be visualised.

The bottom figure of Fig. 5 corresponds to the four images in Fig. 6. It is apparent that a few particles initially leak backwards into the initial feeding chamber, but most eventually feed correctly. These particles begin to climb the pulse-elevator and, by 0.9 s, a large number of particles have already left the device via the spout. The settling chamber above the spout is an iterated design feature that facilitates exit in the context of the wider experimental layout, but it is somewhat outside the scope of this paper.
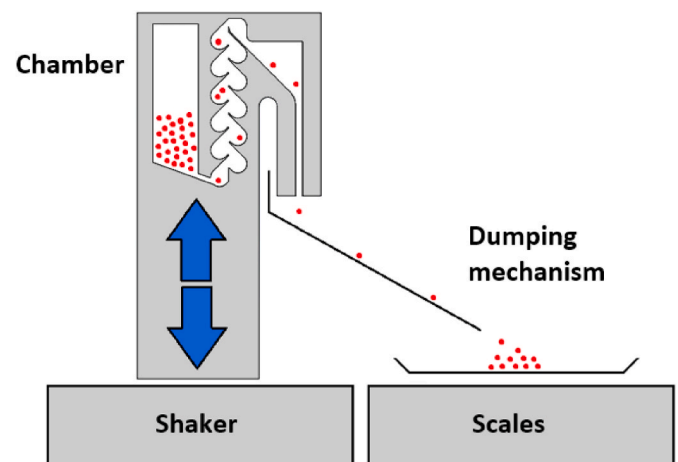

Fig. 7. The experimental setup. Vibration is indicated by the blue arrows, granular material by the red dots. (For interpretation of the references to colour in this figure legend, the reader is referred to the Web version of this article.)

Table 2
Experiments undertaken.

Frequency (Hz)	10	20	30	40	50
1 g	✗	✗	✗	✗	✗
2 g	✓	✗	✗	✗	✗
3 g	✓	✓	✗	✗	✗
4 g	✓	✓	✗	✗	✗
5 g	✓	✓	✓	✗	✗
10 g	✗	✓	✓	✓	✓
15 g	✗	✓	✓	✓	✓
20 g	✗	✓	✓	✓	✓
25 g	✗	✗	✓	✓	✓

5. Experimental results

This geometry is next tested against a range of vibration amplitudes and frequencies, with the measured output being the mass flow rate through the device, using the arrangement in Fig. 7. The geometry analysed in the previous section is 3-D printed to an out-of-the-page depth of 18 mm, and then covered over with a transparent acrylic sheet so that the behaviour inside the device can be observed. There were no significant issues with static attraction to the sheet.

This assembly was then mounted on a shaker (Model-407, LTV LING ALTEC Ltd, Royston, England, UK), so that the required excitation can be applied using a signal generator (Agilent 33220A, Agilent Technologies, Santa Clara, CA, USA) and a power amplifier (PA25E, Electrodynamic LDS, Hottinger Brüel & Kjær, Nærum, Denmark). A little more than 50 g of granular material (1 mm glass beads, illustrated by the red dots) was then loaded into the chamber which feeds the pulse-elevator, via an opening at the top that was closed and resealed with putty.

The granular material is intended to climb from the base of the first scoop to the exit of the last scoop, and then into the spout and on to the weighing scale such that the mass delivered can be measured. The experiments undertaken, with and without success, are shown in Table 2. The maximum accelerations applied ranged from 1 g to 25 g, and the frequencies ranged (as before) from 10 Hz to 50 Hz.

The failed experiments in the upper right of the table were marked unsuccessful (✗) due to their being no measurable output of particles (that is, the system was apparently below the activation threshold), and the failed experiments in the bottom left were marked unsuccessful (✗) because they required amplitudes beyond the operating range of the experimental setup employed. The mass transferred by the successful experiments (✓) was recorded every 5 s, and is presented in Fig. 8, where each data point is in fact the average of three consecutive runs.
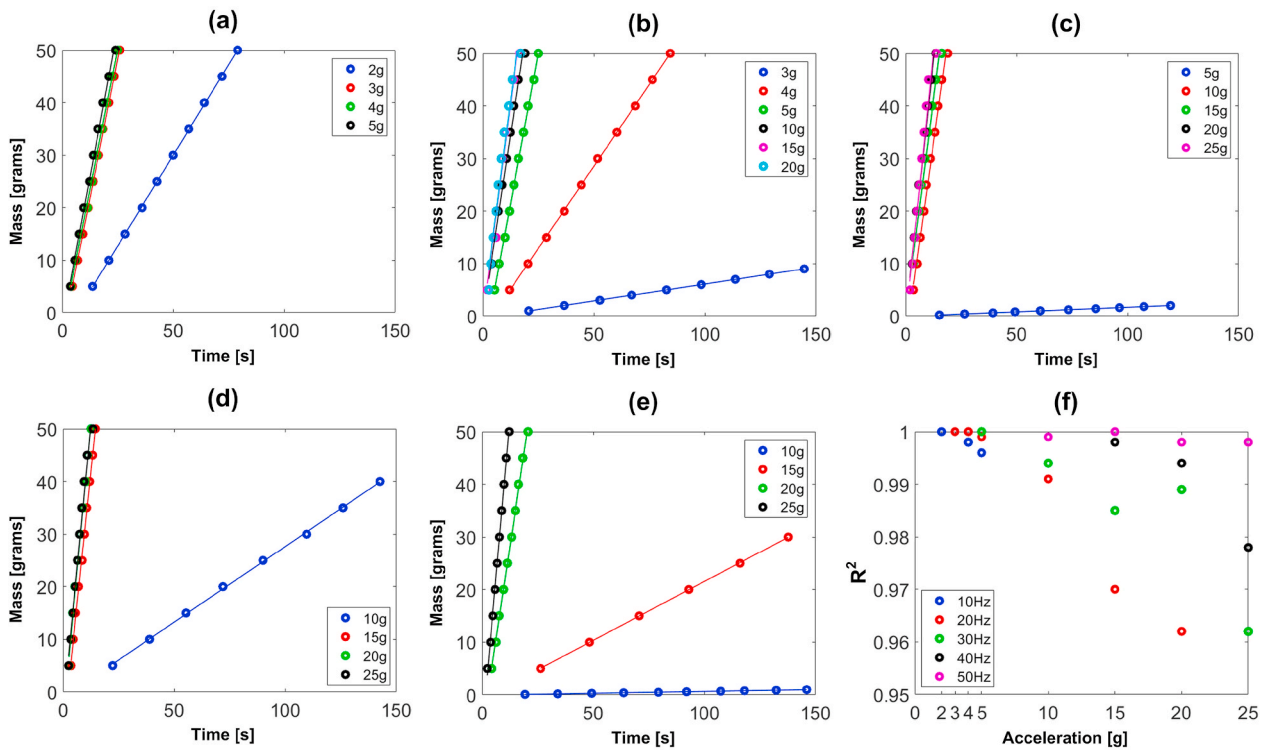
Fig. 8. The experimental performance with glass spheres: (a) 10 Hz, (b) 20 Hz, (c) 30 Hz, (d) 40 Hz, (e) 50 Hz, and (f) R^2 values of the linear trends, where each datapoint on those trends is the average of three runs.

Table 3
Validation of 1-D analytical model for activation and saturation accelerations.

Frequency (Hz)	10	20	30	40	50
Act. 1-D analytic [g]	1.9	3.3	5.2	7.6	10.9
Act. expt. lower bound [g]	1	2	4	5	5
Act. expt. upper bound [g]	2	3	5	10	10
Sat. 1-D analytic [g]	2.4	4.8	8.2	13.1	19.4
Sat. expt. lower bound [g]	2	4	5	10	15
Sat. expt. upper bound [g]	3	5	10	15	20

Note the extraordinary linearity in the performance of the system. This creates some confidence that the pulse-elevator may have some value in particulate metering, as well as the bulk transport applications primarily considered in this paper.

These results can validate the activation and saturation accelerations calculated in Table 1, by setting experimental lower and upper bounds according to the first example of either state. This is a coarse tool, given that the runs were widely spaced in g, but it is nonetheless informative. The result of this analysis is presented in Table 3.

In considering this table, we note that the activation state is easy to define: it is simply a measure of whether an any granular material is ejected, or not. The saturation state is more difficult, being a more asymptotic problem (as is apparent from Fig. 8). Therefore an arbitrary definition of saturation was selected, namely the ejection of the entire 50 g charge in 30 s or less. It is apparent that, in seven out of ten cases, the experimental bounds successfully bracketed the analytical predictions. The three exceptions are missed by no more than 10%.

6. Use case #1: uplifting dry sand from a hopper

A modified pulse-elevator is designed, with a lower inlet that uplifts granular material directly from a hopper, and transfers it to a set of scales. Two grades of block paving sand were tested: a 'coarse' material that did not pass a 60-grit sieve (250+ μm), and a 'fine' material that

passed a 60-grit sieve but not a 100-grit sieve (150 μm–250 μm). Fig. 9 shows the geometry of the modified device, with an intake near the bottom. A transparent cover has been added, and a spout has been provided to transfer the material to the scales. The transparent cover has been sealed to the pulse-elevator with glue, which has resulted in a slightly misshapen appearance, but this is a purely cosmetic shortcoming.

These experiments were challenging. Although vibration can fluidise granular materials [18], this was not clearly observed and there was sometimes considerable resistance-to-motion due to compaction of the
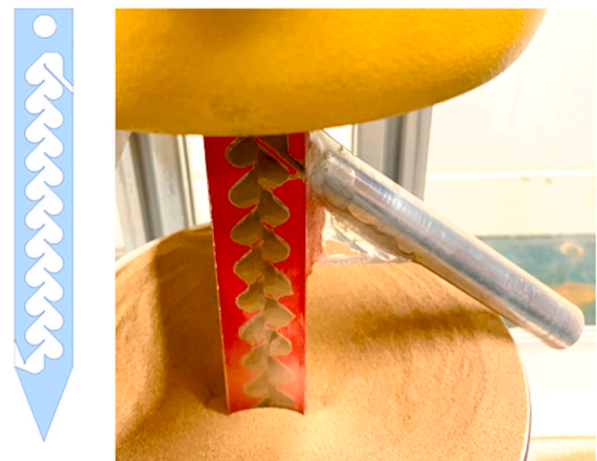

Fig. 9. The experimental setup for uplifting sand, with a red device and a yellow shaker in a bowl of sieved sand. Material flows out of the metal spout when the system is vibrated, at a rate of a few grams per second. Please see the Appendix for a sized drawing of the scoop architecture, which has been applied in a square section. (For interpretation of the references to colour in this figure legend, the reader is referred to the Web version of this article.)

Table 4
Mass of sand (in grams) uplifted from hopper to scales in a 15 s campaign.

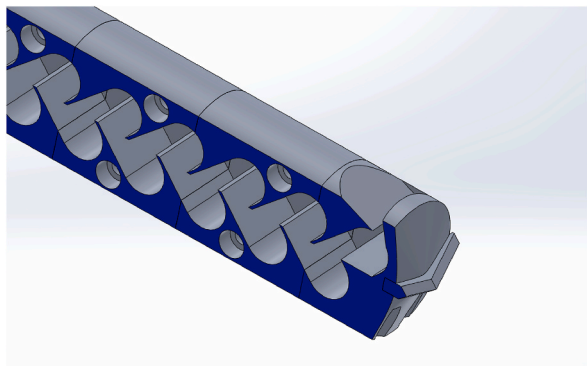| Nominal acceleration setting [g]	20	30
Coarse material [20 Hz]	22.6	–
Coarse material [30 Hz]	12.2	11.5
Fine material [20 Hz]	32.3	10.3
Fine material [30 Hz]	23.0	7.4

Fig. 10. A drillbit containing a pulse-elevator could uplift spoil without gross rotation of the drillbit itself. Please see the Appendix for a sized drawing of this device, which was subsequently manufactured and tested.

granular material under the device. No uplift was seen in the 10 Hz, 40 Hz, and 50 Hz campaigns. However, at 20 Hz and 30 Hz range meaningful and stable throughput was achieved at 20 g and 30 g of nominal acceleration, as per Table 4.

These experiments are not definitive, but rather a functional test to demonstrate that granular materials can be uplifted from a hopper using the pulse-elevator. Although Tesla valves have been suggested as a vibration powered pump for liquid applications [19], we do not believe that this has been previously demonstrated in granular materials.

There is therefore potential for the pulse-elevator architecture to compete with the auger in ISRU applications, for example in elevating large quantities of regolith, particularly if the end-loads can be addressed by a straightforward technique. Torque would not need to be reacted, and the oscillatory loads could be dealt with more easily by means of tuned resonance. The issues of abrasion would be reduced, as sliding particle interactions are reduced, and this may also reduce electrostatic problems. Fines will be transported in vacuum conditions better than they might be on Earth.

7. Use case #2: removing spoil from a drill site without augering

The pulse-elevator geometry could be incorporated into percussive drillbits, as conceived in Fig. 10. These would need to rotate only enough to prevent tooth imprintation, and would uplift spoil from the bottom of the hole using the inlet geometry proven in the previous application before ejecting it above the surface. In this way, it might be possible to drill to a considerable depth without any need to auger the spoil out of the hole.

Given that the auger torque can often be an order of magnitude above the rock-breaking torque [4], this could have a very significant effect on the electromechanical footprint of the drill system as whole.

A rig was constructed to allow a titanium pulse-elevator with a carbide tooth to operate against a block of volcanic tuff, with a small degree of back-and-forth dithering (as opposed to augering) to prevent imprintation of the tooth. This back-and-forth rotation was provided by a Scotch Yoke mechanism operating at a few revolutions per minute, which was powered by a small DC motor. Excitation was provided by an 850 W reciprocating saw (MacAllister MSRS850, B&Q, Eastleigh, England, UK) adapted to hold the pulse-elevator, as shown in Fig. 11. Weight-on-bit was provided by the combined self-weight of the reciprocating saw and the Scotch Yoke assembly (approximately 90 N), which were free to slide on vertical rails. The nominal amplitude was 10 mm and the speed was 45 Hz, for an 81 g acceleration.

This device drilled a 30 mm hole to a depth of 160 mm in the tuff, in 10 min. Spoil was removed from a depth of five bit-diameters without augering or relative movement of any parts downhole, and the slow back-and-forth rotation derived from the Scotch Yoke was apparently entirely sufficient to maintain flow into the device. No choking events were observed. To put this performance into context, a benchmark performance for planetary drill systems is the 1-1-100-100 level, that is, 1 m depth achieved in 1 h, with 100 N weight-on-bit and 100 W of power [20]. The depth, speed, and weight-on-bit metrics are approximately on-target, pro-rata, in this proof-of-concept experiment. However, although it cannot have exceeded 850 W, the power performance is currently unknown.

We are unaware of any cases where this relative depth has been achieved by a mechanical drill system in the absence of an auger or other relatively-moving parts, so there appears to be considerable potential for this alternative architecture. Common issues such as auger choke would be eliminated, but the possibility arises that the scoops could become
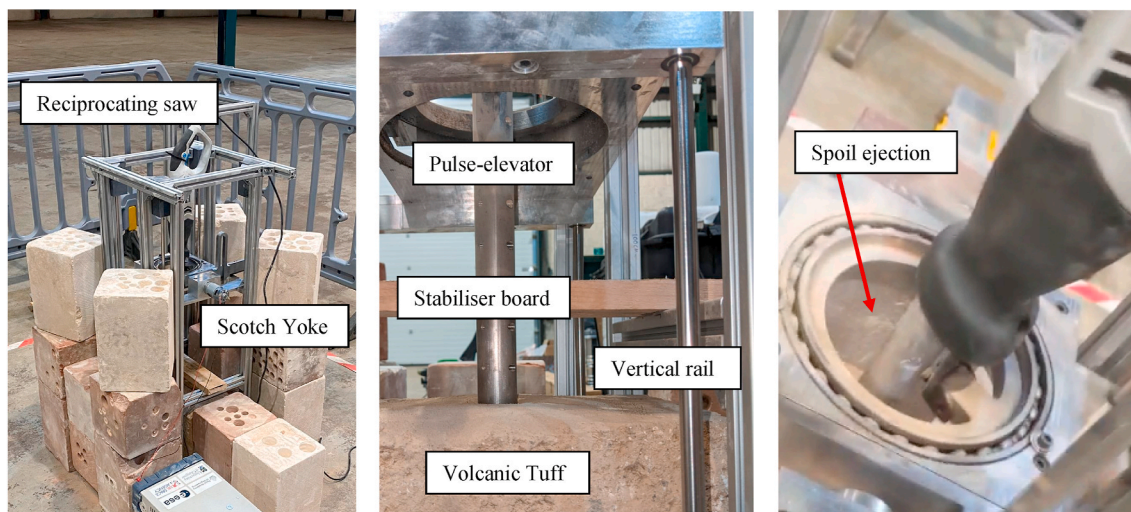

Fig. 11. Left, the saw in the rig, secured against vibration by other blocks. Centre, the pulse-elevator bears down on the tuff block. Right, in operation, spoil (arrowed) can be seen ejecting from the pulse-elevator.

choked instead. This extent to which this can be ameliorated by the shock-loading of the impact events remains to be seen. Furthermore, the need to react torque would be eliminated, bit-walk would be reduced and, because auger power would no longer be required, there may well be energy savings as well.

8. Conclusion

A novel continuous-uplift device, named the pulse-elevator, has been proposed. The operating principle is well-understood, and functional tests in real-world granular materials and hard-rock drilling applications have had positive results. There is a possibility to replace the auger, previously an essential component of planetary drill systems, in some circumstances. The system represents, to the best of our knowledge, the first demonstration of a quasi-Tesla valve in a pumping application, and particularly a vertical application, with respect to a granular material.

Declaration of competing interest

The authors declare that they have no known competing financial interests or personal relationships that could have appeared to influence the work reported in this paper.

Appendix A

The authors believe that anyone wishing to examine this concept may find it helpful to have access to the precise geometry used. One half of the pulse-elevator drillbit is therefore provided below (although the tooth is omitted).
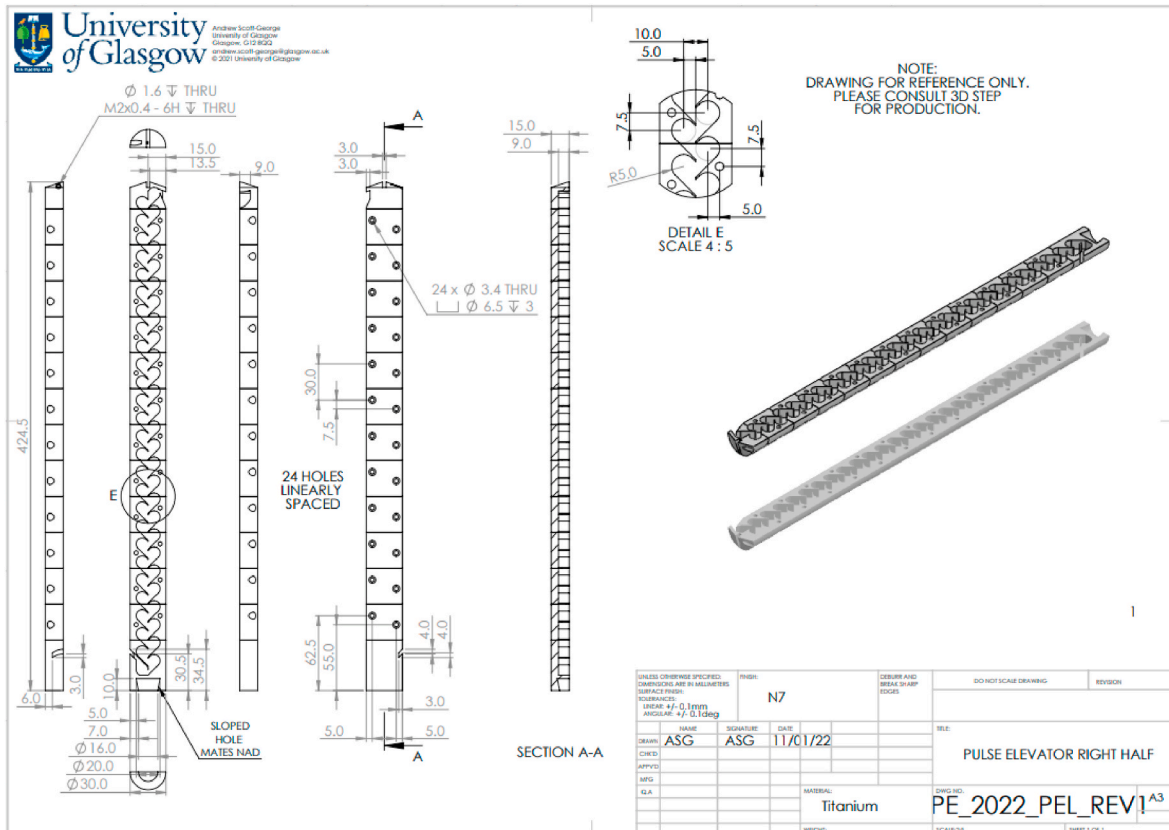
Appendix B. Supplementary data

Supplementary data to this article can be found online at https://doi.org/10.1016/j.actaastro.2022.07.052.

References

[1] J. Benedi, G. Just, M. Roy, K. Smith, A novel approach to the analytical modelling of an auger conveyor system for lunar regolith transportation, Acta Geotech. (2022), https://doi.org/10.1007/s11440-022-01527-3.

[2] Y. Tian, P. Yuan, F. Yang, J. Gu, M. Chen, J. Tang, Y. Su, T. Ding, K. Zhang, Q. Cheng, Research on the principle of a New Flexible screw conveyor and its power consumption, Appl. Sci. 8 (7) (2018).

[3] M. Bortolamasi, J. Fottner, Design and sizing of screw feeders, in: International Congress for Particle Technology, Nuremberg, German, March, 2001.

[4] K. Zacny, G. Cooper, Methods for cuttings removal from holes drilled on Mars, MARS Int. J. Mars Sci. Explor. 3 (2007) 42–56.

[5] K. Zacny, M. Quayle, M. McFadden, A. Neugebauer, K. Huang, G. Cooper, A novel method for cuttings removal from holes during percussive drilling on Mars, in: Revolutionary Aerospace Systems Concepts - Academic Linkage (RASC-AL), 2002, pp. 1–15.

[6] E. Sloot, N. Kruyt, Theoretical and experimental study of the transport of granular materials by inclined vibratory conveyors, Powder Technol. 87 (3) (1996) 203–210.

[7] G. Just, K. Smith, K. Joy, M. Roy, Parametric review of existing regolith excavation techniques for lunar in Situ Resource Utilisation (ISRU) and recommendations for future excavation experiments, Planet. Space Sci. 180 (2020) 104746.

[8] P. Harkness, C. Houston, C. Souza, R. Timoney, K. Worrall, J. Rix, A. Dixon, The DEEPER project: A testbed for 20m scale drilling technologies, in: 16th Symposium on Advanced Space Technologies in Robotics and Automation, ESTEC, 2022.

[9] D. Crouch, Final Report for Apollo Lunar Surface Drill, 1968. Martin Marietta Engineering Report No. ER 14778, NASA-CR-92412.

[10] K. Zacny, G. Paulsen, M. Szczesiak, J. Craft, P. Chu, C. McKay, B. Glass, A. Davila, M. Marinova, W. Pollard, W. Jackson, LunarVader: development and testing of lunar drill in vacuum chamber and in lunar analog site of Antarctica, J. Aero. Eng. 26 (1) (2013) 74–86.

[11] Y. Qian, L. Xiao, S. Yin, M. Zhang, S. Zhao, Y. Pang, J. Wang, G. Wang, J. Head, The regolith properties of the Chang'e-5 landing region and the ground, Icarus 337 (2020), 113508.

[12] M. Litvak, A. Nosov, T. Koslova, V. Mikhal'skii, A. Perkhov, V. Tret'yakov, Deep-hole soil-sampling tools for future Russian lunar polar missions, Sol. Syst. Res. 54 (2020) 203–222.

[13] K. Zacny, et al., Development of Venus drill, in: IEEE Aerospace Conference, Big Sky, Montana, 2017.

[14] R. Moeller, et al., The sampling and caching subsystem (SCS) for the scientific exploration of Jezero crater by the Mars 2020 Perseverance Rover, Space Sci. Rev. 217 (5) (2021).

[15] P. Magnani, E. Re, S. Senese, F. Rizzi, A. Gily, P. Baglioni, The drill and sampling system for the ExoMars Rover, in: International Symposium on Artificial Intelligence, Robotics and Automation in Space, Sapporo, Japan, 2010.

[16] P. Di Lizia, F. Bernelli-Zazzera, A. Ercoli-Finzi, S. Mottola, C. Fantinati, E. Remetean, B. Dolives, Planning and implementation of the on-comet operations of the instrument SD2 onboard the lander Philae of Rosetta mission, Acta Astronaut. 125 (2016) 183–195.

[17] N. Tesla, US Patent 1,329,559, 1920.

[18] D. Firstbrook, Ultrasonically Assisted Penetration through Granular Materials for Planetary Exploration, University of Glasgow, 2017 (PhD Theses).

[19] Q.M. Nguyen, J. Abouezzi, L. Ristroph, Early turbulence and pulsatile flows enhance diodicity of Tesla's macrofluidic valve, Nat. Commun. 12 (2021) 2884.

[20] K. Zacny, G. Paulsen, C. McKay, B. Glass, A. Dave, A. Davila, M. Marinova, B. Mellerowicz, J. Heldmann, C. Stoker, N. Cabrol, M. Hedlund, J. Craft, Reaching 1 m deep on Mars: the icebreaker drill, Astrobiology 13 (12) (2013).